Dev Dynamics
DOI10.1002/dvdy.428

A systematic expression analysis of Plasticity-Related Genes in mouse brain development brings PRG4 into play

Isabel Gross[1,2], Tabea Tschigor[1], Angelina L. Salman[1], Fan Yang[3], Jiankai Luo[3], Danara Vonk[1,4], Mark S. Hipp[4,5], John Neidhardt[6,7] and Anja U. Bräuer[1,2,7,8*]

1.) Research Group Anatomy, School of Medicine and Health Sciences, Carl von Ossietzky University Oldenburg, Oldenburg, Germany
2.) Institute of Anatomy, University Medical Center Rostock, Rostock, Germany
3.) Translational Neurodegeneration Section "Albrecht Kossel", Dept. of Neurology, University Medical Center Rostock, Rostock, Germany
4.) Department of Biomedical Sciences of Cells and Systems, University Medical Center Groningen, University of Groningen, Groningen, The Netherlands
5.) School of Medicine and Health Sciences, Carl von Ossietzky University Oldenburg, Oldenburg, Germany
6.) Human Genetics, Faculty of Medicine and Health Sciences, University of Oldenburg, Oldenburg, Germany
7.) Research Center Neurosensory Science, Carl von Ossietzky University Oldenburg, Oldenburg, Germany
8.) Institute of Cell Biology and Neurobiology, Center for Anatomy, Charité–Universitätsmedizin Berlin, Berlin, Germany

***Corresponding:**

Prof. Dr. Anja U. Bräuer

Fakultät für Medizin und Gesundheitswissenschaften
Carl von Ossietzky Universität Oldenburg

Department für Humanmedizin

Abteilung Anatomie
Carl-von-Ossietzky Str. 9-11
26129 Oldenburg - D

Tel.: +49 (0)441 798 3797

anja.braeuer@uni-oldenburg.de

ORCiD ID: 0000-0003-3651-1470

Accepted Articles are accepted, unedited articles for future issues, temporarily published online in advance of the final edited version.© 2021 Wiley Periodicals, Inc.
Received: Apr 26, 2021;Revised: Aug 24, 2021;Accepted: Sep 20, 2021

Running title

PRGs in mouse brain development

Keywords

PRGs, mRNA expression, primary brain cells, cell morphology, filopodia

Key findings:

- *Prg1*, *-2*, *-3* and *-5* are dynamically expressed during mouse brain development
- *Prg4* shows continuously high expression throughout development and in different brain areas
- *Prgs* are differentially expressed in glial cells
- *Prg3* expression alters during oligodendrocyte maturation
- Unlike close family members, PRG4 does not induce filopodia outgrowth and is not localized to the filopodia plasma membrane

Funding

This work was supported by the funding of I.G.'s work by the FAZIT Stiftung.

Parts of this study were funded by the Verbund Norddeutscher Universitäten to A.U.B. and M.H.

Conflict of interest

The authors declare that they have no competing interests.

Developmental Dynamics

Abstract

Background: Plasticity-Related Genes (*Prgs*/PRGs) or Lipid Phosphate Phosphatase-Related Proteins (LPPRs) comprise five known members, which have been linked to neuronal differentiation processes such as neurite outgrowth, axonal branching, or dendritic spine formation. PRGs are highly brain-specific and belong to the lipid phosphate phosphatases (LPPs) superfamily, which influence lipid metabolism by dephosphorylation of bioactive lipids. PRGs, however, do not possess enzymatic activity, but modify lipid metabolism in a way that is still under investigation.

Results: We analyzed mRNA expression levels of all *Prgs* during mouse brain development, in the hippocampus, neocortex, olfactory bulbs, and cerebellum. We found different spatio-temporal expression patterns for each of the *Prgs,* and identified a high expression of the uncharacterized *Prg4* throughout brain development. Unlike its close family members PRG3 and 5, PRG4 did not induce filopodial outgrowth in non-neuronal cell lines, and does not localize to the plasma membrane of filopodia.

Conclusion: We showed PRG4 to be highly expressed in the developing and the adult brain, suggesting that it is of vital importance for normal brain function. Despite its similarities to other family members, it seems not to be involved in changes of cell morphology; instead, it is more likely to be associated with intracellular signaling.

Introduction

The five known Plasticity-Related Genes (*Prgs*/PRGs), also named Lipid Phosphate Phosphatase Related Proteins (LPPRs), form their own brain- and vertebrate-specific subgroup within the lipid phosphate phosphatase (LPP) protein superfamily [1, 2]. LPPs are surface-located, membrane-spanning proteins with six transmembrane regions and three extracellular loops. These loops contain conserved ecto-enzymatic active sites that dephosphorylate bioactive lipid substrates such as lysophosphatidic acid (LPA) or sphingosine-1-phosphate (S1P) [3-5]. This regulates the affinity of these extracellular lipids to their receptors and thereby modulates the associated intracellular signaling processes.

The PRGs are homologs of LPPs, but they lack the characteristic ecto-phosphatase activity because of non-conserved substitutions in the respective catalytic domains [2, 4, 5]. Regardless of the absent phosphatase activity, PRGs can still influence bioactive lipids and their signaling pathways, but the underlying mechanisms are currently under investigation [6-8]. PRG1 and 2 have about 400 amino acid long C-termini, whereas PRG3, 4, and 5 have rather short ones, consisting of only around 50 amino acids [9]. They differ considerably in their unique intracellular C-termini, which therefore might play a role in mediating their specific functions. For PRG5, for example, a C-terminal binding to phosphorylated phosphatidylinositols (PtdInsPs) has been demonstrated, and its functionality has been linked to this specific interaction [7].

Previous studies have demonstrated a widespread involvement of PRGs in molecular mechanisms of neuronal differentiation. PRG1 was the first PRG identified in a screening of a cDNA library of the lesioned murine hippocampus [1], and remains to date the most-studied PRG. It was shown to be expressed during axonal outgrowth after a

lesion, and to attenuate LPA-mediated axon collapse, hence promoting regenerative sprouting processes [1, 10]. PRG2 has the greatest resemblance to PRG1, and it was functionally correlated to axonal growth and branching by its stabilizing of phosphoinositides in the plasma membrane during brain development [8]. It was also shown to be important for axonal guidance of thalamocortical fibers by its arbitrating of the axonal sensitivity to LPA [11]. The highly homolog PRG3 and PRG5 have both been linked to morphological changes, more precisely to the induction of membrane protrusions such as filopodia [12-14]. In primary cultured neurons, PRG3 overexpression leads to increased neurite outgrowth and neurite shaft protrusion, and was associated with regeneration after spinal cord injury in adult mice [15, 16].

PRG5, however, is assumed to be involved in the formation of dendritic spines, as well as in the morphology, stabilization, and proper function of excitatory synapses [7]. PRG4 has not been specifically analyzed and no functional data is yet available. In a screen of drug-resistant human melanoma cell lines, it was found to be upregulated, but a direct link to lipid phosphate signaling was not observed [17]. The existing information on PRG function implies a central role of this protein class in neuronal development, as well as in neuronal reorganization processes. Furthermore, this can be of use in understanding pathogenesis and associated repair mechanisms. It is therefore of vital importance to further investigate PRG expression and function, including the previously uninvestigated PRG4 protein.

All PRGs show vertebrate- and brain-specific expression. Most previous studies focused mainly on single PRGs, and expression analysis was limited to the corresponding research subject. Here, we aimed for a systematic expression analysis of all known PRGs. We focused on mouse brain development, from late embryonic stages to adulthood, and on different brain-cell types. Our analysis revealed dynamic

expression patterns for *Prg1*, *2*, *3,* and *5.* By contrast, *Prg4* showed high expression levels throughout brain development, raising questions about its specific role in fundamental neuronal processes. In contrast to the closely related PRG3 and PRG5, we found that the overexpression of PRG4 does not induce membrane protrusion and filopodia formation, suggesting a role in a different pathway.

Results

Prgs are dynamically expressed in different brain areas during development

A previous study of the developmental mRNA expression of *Prg3* and *Prg5* in the hippocampus demonstrated a dynamic expression regulation for both *Prgs* [7, 16]. To our knowledge, no systematic gene expression analysis of all *Prgs* during mouse brain development has yet been carried out. Therefore, in this study, we aimed for a complete comparison of the gene expression of all five known *Prgs* in different brain areas. We analyzed mRNA expression levels in the hippocampus, neocortex, olfactory bulbs, and the cerebellum at developmental stages E14 to P30 by qRT-PCR. We found all of the *Prgs* expressed in all analyzed brain regions and developmental stages, but with different dynamic expression patterns (Fig.1, A, C, E, G). The previously published *Prg3* and *Prg5* expression in the hippocampus is included in Figure 1A in shaded bars as a matter of completeness. For direct comparison of pre- and postnatal expression dynamics, we normalized expression levels to P0 expression and plotted changes of all *Prgs* together over time for each brain region (Fig.1, B, D, F, H).

Complementary expression of *Prg1* and *Prg2*

Prg1 expression in the hippocampus, neocortex, and olfactory bulbs increased with progressing development and stayed at high expression levels in adult stages (Fig.1 A-F; E14 vs. P30: hippocampus *** $p = 0.0001$, neocortex *** $p = 0.0002$, olfactory bulbs *** $p < 0.0001$). The cerebellum showed lower *Prg1* expression levels and was the only brain area analyzed in which *Prg1* expression decreased towards adult stages (Fig.1 G -H; P0 vs. P30, *** $p = 0.0002$).

In the hippocampus and neocortex, *Prg2* expression peaked around birth, and strongly declined after P5 (Fig.1 A-D; E14 vs. P0: hippocampus *** $p = 0.0006$, neocortex * $p =$

0.024; P0 vs. P30: hippocampus *** $p < 0.0001$, neocortex *** 0.0001). In the cerebellum, we found a similar expression pattern, but with higher expression levels in very early developmental stages (Fig.1 G-H; E14 vs. P0 not significant, P0 vs. P30 *** $p = 0.0012$). Also, in the olfactory bulbs, the *Prg2* expression did not peak in early development and it stayed at more elevated levels in adulthood, compared to the other analyzed brain regions (Fig.1 E-F; E14 vs. P0 not significant, P0 vs. P30 *** $p = 0.004$).

Our results show complementary expression levels for *Prg1* and *Prg2* during brain development, especially in the hippocampus, neocortex and olfactory bulbs. Expression differences in adulthood were particularly high in hippocampus and neocortex samples.

Temporally shifted expression of *Prg3* and *Prg5*

In-situ hybridization of *Prg3* mRNA in the developing rat brain showed *Prg3* expression from E16, mainly in the hippocampal anlage, thalamus, and the olfactory bulbs [18]. Our qRT-PCR experiments in different areas and different developmental stages of the mouse brain revealed high *Prg3* mRNA expression from developmental stage E14 on in all investigated areas. Expression peaked at late embryonic stages and around birth and decreased to low expression levels in adult stages (Fig.1; E14 vs. P0: hippocampus *** $p < 0.0001$, neocortex *** p = 0.01, olfactory bulbs *** $p = 0.0036$, P0 vs. P30: all areas *** $p < 0.0001$). Only in the cerebellum, we found higher *Prg3* expression in early embryonic development and expression was absent in adult stages (Fig.1 G; E14 vs. P0: not significant, P0 vs. P30: *** $p < 0.0001$). In the olfactory bulbs, *Prg3* expression remained slightly elevated in adult stages compared to the other brain areas. This was also observable for *Prg5*, were expression in the olfactory bulbs did not decrease towards adult stages (Fig.1 E; P0 vs. P30: not significant). However, *Prg5* expression peaked later, in early postnatal stages, resulting in a slightly shifted

expression pattern of these genes (E14 vs P0: all areas *** $p < 0.0001$; P0 vs. P30: hippocampus, neocortex and cerebellum *** $p < 0.01$). Our results show similar expression patterns for *Prg1* and *Prg5* genes, as well as for *Prg2* and *Prg3* genes, albeit at different expression levels (Fig.1 B, D, F, H).

Continuously high expression of *Prg4* throughout brain development

At the time of this study, *Prg4* expression in mouse brain tissue had not been documented in the literature. Here we show its mRNA expression in developing mouse brain areas for the first time (Fig.1). We found *Prg4* to be ubiquitously expressed throughout all developmental stages and all brain areas examined. We found only one significant expression peak, in the neocortex around birth (Fig.1 C; E14 vs. P0 *** $p < 0.0001$) and significant expression decreases towards adulthood in the neocortex and the cerebellum (Fig.1 G; P0 vs. P30: neocortex *** $p < 0.0001$, cerebellum *** $p = 0.0006$). In comparison to other *Prg* family members, only very minor, changes could be detected, and in the hippocampus and the olfactory bulbs its expression remained stable throughout development (Fig.1 B, D, F, H; E14 vs. P30: hippocampus and olfactory bulbs, not significant).

***Prg* expression in different primary brain cells**

Previously, we investigated the expression of *Prg3* and *Prg5* in different primary brain cells (neurons, astrocytes, and microglia) and demonstrated their mainly neuronal expression (Fig. 2 A, shaded bars) [7, 16]. Analysis of *Prg1, 2,* and *4* in these cultured primary neuronal cells also revealed a predominantly neuronal expression. Only *Prg4* additionally showed increased expression in astrocytes, whereas *Prg1, 2,* and *5* were only weakly expressed in this cell type. All *Prgs* are only poorly expressed in microglia, with *Prg2* showing higher expression than the other family members (Fig. 2 A).

We found all *Prgs* to be expressed in primary cultured oligodendrocytes, with high expression levels of *Prg1, 3, 4,* and *5*. Strikingly, *Prg3* was highly expressed in immature oligodendrocytes, but decreased during oligodendrocyte maturation (Fig 2B; immature vs. mature * $p = 0.0294$). *Prg1*, *Prg4,* and *Prg5,* on the other hand, exhibited a high expression in both immature and mature primary cultured oligodendrocytes. *Prg2* was the least expressed *Prg* in oligodendrocytes, with a slight, but not significant decrease towards maturation (Fig. 2 B).

Amino acid sequence alignment of murine PRG3, PRG4 and PRG5 proteins

To analyze whether the gene expression pattern can be linked to structural similarities, we aligned murine amino acid (aa) sequences of all family members. PRG1 and PRG2 show 49.1 % aa sequence identity, whereas their resemblance to other PRGs varied between 36.01 % and 40.94 %. We found the highest similarity between PRG3 and PRG5, with 55.24 % aa sequence identity. The uncharacterized PRG4 protein most closely resembled PRG3 and 5, with 49.04 % and 50.97 % identity, respectively, and only weakly resembled PRG1 and 2, with 34.42 % and 36.01 % respectively (Table 2).

Table 2: Amino acid identity from pairwise comparison of murine PRGs

	% Identity				
Protein, Accession no.	**PRG1**	**PRG2**	**PRG3**	**PRG4**	**PRG5**
PRG1, Q7TME0	100				
PRG2, Q7TPB0	49.1	100			
PRG3, Q8BFZ2	40.94	37.65	100		
PRG4, Q8VCY8	34.42	36.01	49.04	100	
PRG5, Q8BJ52	37.36	38.75	55.24	50.97	100

Due to their high aa sequence identity, we aligned murine PRG3, 4 and 5 aa sequences to localize differences within the proteins (Fig. 3). We found the largest differences in the intracellular N- and C-termini, the first intracellular loop (ICL), and the second extracellular loop (ECL) of the proteins. The intracellular N-terminus of PRG5 is very short and consists of five aa less than that of PRG3, and six aa less than the N-terminus of PRG4. PRG3 and PRG4 N-termini are longer, but do not share sequence similarities.

The second ECL of PRG4 consisted of 7 aa more than that of PRG3 and 5, and thus differs distinctly. All three PRGs share an N-glycosylation side in the loop that is required for membrane insertion, as shown for PRG3 by Velmans et al. 2013. PRG4 has a 7 aa longer C-terminus than both PRG3 and 5. Domain similarities at the C-terminus of the three proteins can only be seen at the passage from the transmembrane region 6 (TM6) to the intracellular C-terminus. The additional aa in the N- and C-termini and the second ECL of PRG4 make it, with 343 aa, the longest of these three PRGs. Despite the about 50% identity in the aa sequence, PRG4 shows distinct differences in protein areas that might be crucial for its specific function. To analyze possible signal peptides in PRG sequences, we used the SignalP 5.0 online tool (https://services.healthtech.dtu.dk/service.php?SignalP-5.0) [19]. Interestingly, none of the PRGs is likely to have a known signal peptide at its N-terminus, or first transmembrane region. Hence, insertion of PRGs into the membrane might underly a different, as yet unknown, mechanism.

Unlike PRG3 and PRG5, PRG4 does not induce filopodial outgrowth in non-neuronal cells

Overexpression of PRG3 and PRG5 has been demonstrated to lead to similar phenotypes in neuronal and non-neuronal cell lines [12-14, 18]. These phenotypes are

marked by intense formation of actin-rich membrane protrusions that were identified as filopodia. Due to their high aa sequence identity, we investigated whether PRG4 induces a comparable phenotype in non-neural cell lines. We identified strong filopodial formation after PRG3 and PRG5 overexpression in HEK293H cells (Fig. 4) and therefore chose this cell line for the analysis of PRG4 overexpression. We know of no reliable antibody against PRG4 and therefore used N- and C-terminal eGFP fusion proteins and C-terminal FLAG-tagged proteins for transfection experiments. All PRG4 constructs were unable to induce the pronounced formation of membrane protrusions and filopodia-like structures seen for PRG3 and PRG5 eGFP and FLAG-tagged constructs (Fig. 4). We observe a mainly intracellular localization of the PRG4 fusion proteins, with only few areas of plasma membrane localization, mainly restricted to central areas of the cell (Fig. 4 B). Quantification of filopodia formation, by determining the number of filopodia per cell, supported the immunostaining results and showed significant differences between PRG3 and PRG5 compared to PRG4 overexpressing cells (Fig. 4 C).

Surprisingly, the N-terminal fusion of eGFP to PRG5 disabled the induction of filopodial formation by PRG5. This was not the case for PRG3, where N- and C-terminal fusion proteins where able to promote filopodial outgrowth. For PRG4, no differences between fusion sites were observed (Fig. 4 B).

Cooperative expression of PRG3, PRG4, and PRG5 in HEK293H cells

Using co-immunoprecipitation and co-localization analysis, Yu et al. showed cooperative interactions of PRG3 with its family members PRG1, PRG2, and PRG5. They demonstrated that the co-expression of PRG3 and PRG5 facilitated their localization to the plasma membrane, particularly to membrane protrusions and filopodia, and also increased membrane protrusion outgrowth [13]. We examined

whether the localization of PRG4 to the filopodia plasma membrane is dependent on an interaction with its close family members PRG3 and PRG5, and if this interaction might be necessary for a possible phenotype of PRG4 overexpression. We therefore generated a PRG4-FLAG construct, which showed equivalent results to the eGFP constructs before, and when co-transfected PRG4 with PRG3 or PRG5 in HEK293H cells. Figure 5 shows HEK293H cells, co-transfected with the PRG4-FLAG and either PRG3-eGFP (A), PRG5-eGFP (B) or a CFP-MEM vector as a control membrane protein (C). Both family members failed to increase localization of PRG4 to the filopodia plasma membrane (Fig. 5, white arrow heads), which mainly remained localized to intracellular structures and central plasma membrane areas. Both PRG3 and PRG5 showed intracellular co-localization with PRG4. The PRG3- and PRG5-specific phenotypes of increased filopodial outgrowth were not altered by additional PRG4 overexpression and could still be observed after co-transfection (Fig. 5 A, B). The same results were obtained with co-transfection of PRG4-eGFP with PRG3- or PRG5-FLAG constructs (data not shown), and co-transfection with CFP-MEM control vector did not affect the overall distribution patterns (Fig.5 C).

Discussion

In this study, we examined the gene-expression profiles of all *Prg* family members during mouse brain development, in the hippocampus, neocortex, olfactory bulbs, and the cerebellum, from embryonic stage E14 to maturation at P30. Our results showed different temporally and spatially dependent dynamic expression patterns for each of the *Prgs*. Our data fit well to previous functional studies on *Prgs,* and can also be used for further analysis, as expression patterns can be linked to specific developmental processes at distinct stages.

Functional studies on PRG1 indicate its involvement in axonal outgrowth [1, 10] and glutamatergic transmission at the postsynapse [6, 20]. These processes are associated with late embryonic and early postnatal development, where we found the highest *Prg1* expression levels.

Our results on *Prg2* expression are in line with recent results on developmental protein expression in total rat brain lysates, with an expression peak around birth and low expression levels in mature stages [8]. Additionally, we showed that *Prg2* remains at elevated levels in the adult olfactory bulbs. *Prg2* has been correlated to axonal and dendritic branching processes of cortical neurons *in-vitro* by inhibition of PTEN and the resulting stabilization of $PI(3,4,5)P_3$ [8]. We detected *Prg2* mRNA expression in embryonic and early postnatal stages that are linked to neuronal migration and branching processes, especially of axonal projections. Elevated *Prg2* expression in the olfactory bulbs could be explained by the olfactory bulb's regenerative and re-wiring capacity in adulthood, which might require PRG2/PTEN interaction in axonal branching processes.

Several studies of *Prg3* expression and function exist. Savaskan et al. analyzed *Prg3* mRNA expression in rat brain and found similar expression patterns to the current

study, with high levels in late embryonic stages and an expression decline after birth. In adult stages, they reported high *Prg3* expression in the hippocampus; additionally, we found high expression in adult olfactory bulbs [18]. Wang and Molnar analyzed *Prg3* expression in mice, specifically in the cerebral cortex, and found differential expression between cortical layers. They describe a decline in differential expression after P10, which matches the general drop in *Prg3* expression of our analysis [21]. The PRG3 protein was reported to influence cell morphology by inducing membrane protrusions in different cell lines, and *Prg3* knock-down decreases the number of neurites in primary cultured neurons [14, 16, 18]. In line with these findings, stages of high *Prg3* expression can be linked to neuronal branching processes during development.

The closely related PRG5 protein has also been linked to cell morphological changes in different cell lines. Overexpression in primary cultured neurons leads to the premature formation of spine-like structures, and to an increased spine density and altered spine morphology in mature neurons [7]. We found *Prg5* expression in stages of synapse formation and maturation, around birth and during early postnatal development. We also identified *Prg5* expression as remaining elevated in regions of high neuronal plasticity: the hippocampus and the olfactory bulbs. This indicates a possible participation of the PRG5 protein in adult neuronal plasticity, which includes morphological changes in synaptic connections.

No expression studies for *Prg4* have been conducted so far, and to date, almost no functional data is available. The only published data, from Tanic et al., identified *Prg4* overexpression in a screening of differentially expressed genes in drug-resistant melanoma cells [17]. We found *Prg4* to be highly expressed during development of the hippocampus, neocortex, olfactory bulbs, and the cerebellum. Expression levels were remarkably stable during the explored time period and were not linked to specific

developmental processes. This suggests a role of *Prg4* in basic neuronal or cellular functionality, and makes its further investigation, including under pathological conditions, particularly interesting.

All *Prgs* are most highly expressed in primary cultured neurons, compared to astrocytes and microglia. We showed that all *Prgs* are also expressed in oligodendrocytes with different dynamic regulations during oligodendrocyte maturation. Especially *Prg3* showed a significant expression decrease in mature oligodendrocytes compared to immature ones. *Prg4* and *5* on the other hand show strong and stable expression levels. Previous studies showed axonal expression of PRG1, 2, and 3, with links to axonal growth or branching processes [1, 8, 16]. These processes might be supported by additional PRG activity in oligodendrocytes. PRG3 has been shown to counteract neurite growth inhibitors, and to reduce myelin- and RhoA-mediated axon collapse [15]. Our data show that further investigation of PRG function in oligodendrocytes could be of specific interest, especially for PRG3, which may be involved in the lack of an axonal regeneration capacity in the mammalian central nervous system.

Amino acid sequence analysis showed the highest similarities of PRG4 to PRG3 and PRG5, but the sequence alignment of these PRGs reveals pronounced differences at the N- and C-termini, and at the first ICL and the second ECL, regions that could be essential for protein functionality. We therefore compared morphological changes induced by overexpression of these PRGs. PRG4 did not show the filopodial formation as seen in PRG3 and PRG5, and we did not identify any other morphological changes after PRG4 overexpression. Additionally, we did not find a localization of PRG4 to the filopodia plasma membrane, but instead mainly to intracellular membranes and plasma membrane areas of the cell body. This was also not affected when PRG4 was co-

transfected with PRG3 or PRG5, whereas it was shown that PRG5 facilitated plasma membrane localization of PRG3 and further increased the induction of membrane protrusions [13]. Also, co-immunoprecipitation results of Yu et al. support direct interactions of at least PRG2, PRG3, and PRG5, but did not include PRG4 [13]. Our results do not support a direct functional interaction of PRG4 with its close family members PRG3 and PRG5, but this needs further examination. Notably, the lack of specific and reliable antibodies against PRG proteins impedes functional experiments and interaction studies, and complicates the analysis of native PRGs in tissue. The possibility that the protein tag interferes with the sorting or functionality of the original PRG4 protein is unlikely, as we analyzed PRG4 fusion proteins with different N- and C-terminal protein tags. Also, co-immunostaining with the endoplasmic reticulum (ER) marker calnexin revealed that PRG4 fusion constructs are not retained in the endomembrane system (Data not shown), and thus indicating proper protein folding and transport.

Our results indicate that PRG4 has a different function to PRG3 and 5. PRG5 was found to interact with PtdInsPs via its C-terminus, and this is required for the induction of membrane protrusions [7]. We found PRG4 to be localized to intracellular membranes and only much less to the plasma membrane. This suggests a prospective involvement of PRG4 with intracellular lipid metabolism rather than an interaction with plasma membrane lipids. The functional role of the PRG4 C-terminus in protein sorting, and in interactions with phospholipids has to be evaluated.

Interestingly, we found that the site of a protein tag at a PRG can affect its functionality. The N-terminal fusion of eGFP to PRG5 prevented its localization to the plasma membrane and, consequently, the induction of filopodial formation. We did not observe this for PRG3 constructs, where both the N-terminal and C-terminal eGFP had no

influence on its observable function. The N-terminus, particularly, differs between PRG3, 4, and 5, and PRG5 has a very short N-terminus, only five amino acid long. Because of this very small size, it is possible that a tag could disturb its proper insertion into the membrane. Nevertheless, a specific role of each N-terminus cannot be ruled out, and remains to be individually elucidated. Our results show that protein tags can influence protein function or interaction, and that this should be considered when analyzing PRG function.

Conclusion

During mouse brain development, *Prgs* show specific and highly dynamic expression levels. Expression levels can be directly linked to existing functional data of each PRG, and the expression pattern can be of help in further functional analysis. We demonstrated that the uncharacterized *Prg4* is regulated differently, and is highly expressed during mouse brain development, and in all analyzed brain areas. Although PRG4 displays a high degree of similarity to PRG3 and PRG5, it is retained within the secretory pathway and does not induce morphological changes like filopodial outgrowth. The localization of PRG4 to intracellular membranes indicates a possible involvement in intracellular lipid metabolism.

Experimental Procedures

Animals

To obtain qPCR samples of staged brain development and primary neurons, astrocytes, and microglia, timed-pregnant, postnatal, and adult C57BL/6 mice were obtained from the Charité – Universitätsmedizin central animal facility (FEM). Postnatal BALB/c mice were used for oligodendrocyte preparations and were obtained from the central animal facility of the University Medical Center in Rostock. Mice were kept under standard laboratory conditions (12-hour light/dark cycle; 55% +/- 15% humidity; 22°C +/- 2°C room temperature, and water ad libitum, enriched and grouped) in accordance with German and European guidelines (2010/63/EU) for the use of laboratory animals. Approval of experiments was obtained from the local ethics body of Berlin (LAGeSO: T0108/11) and Mecklenburg-Vorpommern (LALLF). For primary cell culture preparation, the day of the vaginal plug following mating was assigned as embryonic day 0.5 (E0.5). Experiments were performed on E16, E18, and E19 embryos and perinatal pubs (postnatal day 0, P5, P10, P15, P20, and P30). Sample and animal numbers were defined as “n” for the number of independent preparations carried out and “N” for the total amount of animals used.

RNA extraction, cDNA synthesis and quantitative real-time PCR (qRT-PCR)

Postnatal and adult mice were sacrificed by cervical dislocation, and early postnatal and embryonic mice by decapitation. Neocortex, hippocampus, cerebellum, and olfactory bulbs of the developmental stages embryonic day (E) 14, E16, E19, and of postnatal days (P) 0, P5, P10, P15, P20, and P30 were dissected out and immediately snap-frozen. For embryonic stages, tissue samples of all embryos of one litter (7 to 10 embryos; N = 21 – 30, sex not specified) were pooled, and three independent litters (n

= 3) were used. Sexes of embryos were not determined. Postnatal tissue samples were pooled from six mice of both sex and three independent preparations (n = 3) were carried out, resulting in a total of 18 animals for each postnatal developmental stage (N = 18). Primary hippocampal neurons at DIV7, astrocytes and microglia cells at DIV14 to 16, immature oligodendrocytes at DIV3, and mature oligodendrocytes at DIV6 (approximately $3x10^5$ cells for each experiment from 3 independent preparations of 3 pregnant mice) were scraped in 1x PBS, centrifuged for 5 min at 900 g at 4°C. Cell pellets and tissues were homogenized in TRIzol (Thermo Fisher Scientific, Waltham, MA, USA), and total RNA extraction was performed following the manufacturer's instructions. RNA concentrations were determined by spectroscopy using an UV/Vis spectrometer (BioSpectrometer basic, Eppendorf, Hamburg, Germany). For cDNA synthesis, 2.5 µg of total RNA was used for reverse-transcription to single-stranded cDNA with the High Capacity cDNA Reverse Transcription Kit (Thermo fisher Scientific) following the manufacturer's protocol. A control reaction was performed without MultiScribe reverse transcriptase and the quality of the amplified cDNA (with and without MultiScribe reverse transcriptase) was tested using beta-actin *(Actb)* PCR.

Quantitative-RT-PCR was performed using the TaqMan™ Fast Universal PCR Master Mix (2X), No AmpErase™ UNG (Thermo Fisher Scientific) and 96-well optical reaction plates from Applied Biosystems (Thermo Fisher Scientific), or hard-shell 96-Well PCR plates from Bio-Rad Laboratories (Hercules, CA, USA). Reactions were prepared according to the manufacturer's protocols. The TaqMan™ Expression Assays used are listed in Table 3. Reactions contained a TaqMan™ probe (5 µM), a forward primer (18 µM), and a reverse primer (18 µM). TaqMan™ probes were tagged at the 5'-end with the reporter dye FAM (6-carboxyfluorescein) and with a minor groove binder (MGB) attached to a non-fluorescent quencher at the 3'-end. QRT-PCR reactions were

carried out with the ABI PRISM 7700 Sequence Detection System (Thermo Fisher Scientific), the ViiA 7 Real-Time PCR System (Thermo Fisher Scientific), or the CFX96 Touch™ Real-Time PCR Detection System (Bio-Rad Laboratories) using the following cycling parameters: 95 °C for 20 s, 95 °C for 1 s and 60 °C for 20 s, for 45 cycles. Expression data of three independent preparations with duplicates of each reaction were calculated using the ΔCt method, with normalization to *Gapdh* and *Actb* as housekeeping genes [22]. Results with both housekeeping genes revealed similar expression patterns and therefore only data normalized to *Gapdh* is shown in the results. Primary cultured cell samples were validated by qRT-PCR with the following cell-type specific marker genes: neuroblast-specific class III β-tubulin (*Tuj1*) for neurons, glial fibrillary acidic protein (*Gfap*) for astrocytes, ionized calcium-binding adaptor molecule 1 (*Iba1*) for microglia, neuron-glial antigen 2 (*Ng2*) for immature oligodendrocytes, and myelin basic protein (*Mbp*) for mature oligodendrocytes. Oligodendrocyte maturation was verified by statistical analysis of *Ng2* and *Mbp* expression using an unpaired, two-tailed *t*-test (*Ng2*: * $p = 0.0407$; *Mbp*: ** $p = 0.0003$).

Sequence Alignment

The alignment of amino acid sequences for the analysis of sequence similarities was accomplished with the basic local alignment online search tool provided by BLAST®. Figures of aligned sequences were generated with CLC Sequence Viewer 8 software (Qiagen, Hilden, Germany).

Primary cell cultures

For primary neuron culture, hippocampi of 7 to 10 E18 (+/- 0.5 days) mouse embryos from one pregnant mouse were dissected and cultures prepared as previously described (Brewer et al 1993). Neurons were plated onto poly-l-lysine coated plastic ware at a density of 2.1×10^4 cells/cm^2 in Minimal Essential Medium (Thermo Fisher

Scientific) supplemented with 0.6 % glucose, 10 % horse serum, and 100 U/ml penicillin/streptomycin (PAN-Biotech, Aidenbach, Germany). Media were changed after 3 to 4 hours to Neurobasal A media supplemented with 2% B27, 0.5 mM glutamine (all from Gibco, Thermo Fisher Scientific), and 100 U/ml penicillin/streptomycin. Three independent preparations were carried out (n = 3; N = 21 to 30). Sample and animal numbers were defined as "n" for the number of independent preparations carried out and "N" for the total amount of animals used.

For preparation of murine astrocytes and microglia, three to four P0 to P2 mouse pups from the same litter were sacrificed, their neocortex and cerebellum dissected and washed in Dulbecco's Modified Eagle's Medium (DMEM, 4.5 g/L glucose, pyruvate, Thermo Fisher Scientific) containing 10 % fetal bovine serum (FCS), 200 mM L-glutamine, and 100 U/ml penicillin/streptomycin. Sexes of pubs were not determined. Astrocyte and microglia preparation and cultivation was performed as previously described [23] and three independent preparations were carried out (n = 3; N = 9 to 12). Cells were harvested after 14-16 days *in-vitro* (DIV).

Oligodendrocyte cultures were prepared from cerebral hemispheres of three P5 mouse pups from the same litter as described in Suckau et al., 2019. Sexes of pubs were not determined. After seeding of purified oligodendrocytes, the medium was not further changed and immature oligodendrocytes were harvested after 3 days, mature ones after 6 days. Three independent preparations for immature and three independent preparations for mature oligodendrocytes were carried out (n = 3; N = 9).

All primary cell cultures were routinely maintained at 37 °C and 5 % CO_2.

HEK393H cell culture, transfection, and constructs

HEK293H (Thermo Fisher Scientific, catalog ID 11631017) cells were routinely maintained in DMEM (PAN-Biotech) supplemented with 10 % FCS, 200 mM L-glutamine, and 100 U/ml penicillin/streptomycin at 37 °C and 5 % CO_2 and passaged at 80-90 % confluency twice a week.

Cells were transfected using the calcium-phosphate method. Therefore, cells were seeded onto poly-l-lysine coated coverslips in 12-well plates with a density of 30,000 cells/cm^2 and transfected after 24 h: 1 µg plasmid DNA, 25 µl sterile H_2O, 2.5 µl of a 2.5 M calcium chloride solution, and 50 µl Hepes-buffered saline pH 7.05 were mixed and added to one well. After 24 h, cells were fixed for immunostaining. The following expression plasmids were used for transfection: peGFP-N1-rPRG3, peGFP-C1-rPRG3, p3FLAG-CMV7.1-rPRG3 [16, 18], peGFP-N1-mPRG4, peGFP-C1-mPRG4, pFLAG-CMV2-mPRG4 [7, 18], peGFP-N1-rPRG5, peGFP-C1-rPRG5, pcDNA3.1zeo+-3FLAG-mPRG5 [7, 12], and peCFP-MEM (Takara Bio Inc., Clontech, Kusatsu, Japan).

For quantification of filopodia formation, HEK293H cells were co-transfected with the indicated PRG construct and a membrane-targeting CFP (CFP-MEM) for visualizing the overall cell morphology to allow filopodia counting. All CFP marked membrane protrusions ≥ 2 µm of one cell were counted. Data were collected from n = 3 independent transfection experiments with at least 10 cells of each experiment and with N = number of total cells counted.

Immunocytochemistry

After transfection, HEK293H cells were washed twice with 1x PBS, and fixed with 4% paraformaldehyde and 15 % sucrose in 1x PBS for 20 minutes at room temperature (RT). Cell membranes were permeabilized with 0.1 % Triton-X100 and 0.1 % sodium

citrate in 1x PBS for 3 minutes at RT, coverslips were then washed three times with 1x PBS, and non-specific antibody binding was blocked with 10% normal goat serum (Vector laboratories, Burlingame, CA, USA) in 1x PBS for 1 h at RT. Primary antibody incubation was conducted in 5% normal goat serum in 1x PBS overnight at 4°C, followed by three washing steps with 1x PBS, and secondary antibody and 0.5 µg/µl DAPI (Carl Roth, Karlsruhe, Germany) incubation in the same solution as primary antibodies for 2 h at RT. Coverslips were again washed three times with 1x PBS and mounted on microscope slides using Mowiol/DABCO (Carl Roth). The following primary and secondary antibodies and concentrations were used: mouse-anti-FLAG (Merck, Darmstadt, Germany, F3165) 1:1500, rabbit-anti-GFP (abcam, Cambridge, UK, ab6556) 1:2500, goat-anti-mouse-Alexa568 (Thermo Fisher Scientific, A11004), goat-anti-rabbit-Alexa488 (Thermo Fisher Scientific, A11008).

Microscopy

Confocal images of transfected HEK293H cells were acquired as z-stacks with a Leica SP8 upright laser microscope equipped with 40x (oil-immersion, 1.3 NA) and 63x objectives (oil-immersion, 1.4 NA), using sequential scanning with the 488 nm line of an argon-ion laser and the 552 nm line of a helium laser. Images are presented as maximum projections of z-stacks. Orthogonal views, background correction and brightness and contrast adjustments were performed using either LasX software (Leica Microsystems, Wetzlar, Germany) or ImageJ (NIH, Bethesda, MD, USA).

Statistical Analysis

Statistical evaluation of the qRT-PCR results of developmental stages in different brain areas (Fig. 1) and primary cultured cells (Fig. 2A) was performed using a one-way analysis of variance (ANOVA) followed by a Bonferroni's multiple comparisons test. Developmental stages E14, P0 and P30 were chosen for statistical evaluation of

embryonic, birth and adult expression differences. qRT-PCR results of primary oligodendrocyte maturation were analysed with GraphPad Prism 7 by an unpaired one-tailed *t*-test. Data are shown as mean ± SD and were considered significant for $p \leq 0.05$ (* $p \leq 0.05$, *** $p \leq 0.01$). Normal distribution of qRT-PCR results was assessed by the Shapiro-Wilk test for small samples sizes ($p > 0.05$). Quantification of filopodia formation (Fig. 4C) is visualized in a boxplot graph including all data points and was statistically analysed by using a Kruskal-Wallis test followed by a Dunn's multiple comparison test. All statistical analyses and graphs were created using GraphPad Prism 7 (GraphPad Software, San Diego, CA, USA).

Declarations

Acknowledgements

The authors thank Jennifer Sevecke-Rave, Beate Bous, Tanja Velmans, Bettina Brokowski and Rike Dannenberg for the excellent technical assistance. We further thank Dr. Dirk Koczan for his expert help throughout the qRT-PCR analysis. The authors acknowledge the Fluorescence Microscopy Service Unit, Carl von Ossietzky University Oldenburg, for the use of the imaging facilities and the FAZIT Stiftung for financial support. English language services were provided by native speaker Prof. Geoffrey Manley from STELS-OL. Parts of this study were supported by the Verbund Norddeutscher Universitäten to A.U.B. and M.H.

Author's contributions

A.U.B., in cooperation with I.G. designed the study and wrote the paper, with contribution from all co-authors. I.G. performed qRT-PCR of PRGs in oligodendrocytes, statistical analysis of all qRT-PCR results, amino acid sequence analysis and alignments, HEK cell transfection and immunocytochemistry of cooperative PRG expression, confocal image acquisition and image editing. T.T. performed qRT-PCR experiments in brain areas and in neuronal cell types, amino acid sequence analysis and alignments, HEK cell transfection and immunocytochemistry of single PRGs. A.L.S. validated the PRG4-FLAG construct. F.Y. and J.L. prepared and provided oligodendrocyte cultures. J.N. provided the qRT-PCR system and helped with the analysis. D.V. performed statistical analysis of filopodia formation. M.H. revised the manuscript. Other cell cultures, RNA isolation, and cDNA preparation were performed by the acknowledged technical assistants. Data from this work is part of the Bachelor

thesis of T.T., and of the PhD thesis of I.G. All authors read and approved the final manuscript.

References

1. Brauer AU, Savaskan NE, Kuhn H, Prehn S, Ninnemann O, Nitsch R. A new phospholipid phosphatase, PRG-1, is involved in axon growth and regenerative sprouting. *Nat Neurosci*. Jun 2003;6(6):572-8. doi:10.1038/nn1052

2. Brauer AU, Nitsch R. Plasticity-related genes (PRGs/LRPs): a brain-specific class of lysophospholipid-modifying proteins. *Biochim Biophys Acta*. Sep 2008;1781(9):595-600. doi:10.1016/j.bbalip.2008.04.004

3. Brindley DN, English D, Pilquil C, Buri K, Ling ZC. Lipid phosphate phosphatases regulate signal transduction through glycerolipids and sphingolipids. *Biochim Biophys Acta*. May 23 2002;1582(1-3):33-44.

4. Brindley DN. Lipid phosphate phosphatases and related proteins: signaling functions in development, cell division, and cancer. *J Cell Biochem*. Aug 01 2004;92(5):900-12. doi:10.1002/jcb.20126

5. Sigal YJ, McDermott MI, Morris AJ. Integral membrane lipid phosphatases/phosphotransferases: common structure and diverse functions. *Biochem J*. Apr 15 2005;387(Pt 2):281-93. doi:10.1042/BJ20041771

6. Trimbuch T, Beed P, Vogt J, et al. Synaptic PRG-1 modulates excitatory transmission via lipid phosphate-mediated signaling. *Cell*. Sep 18 2009;138(6):1222-35. doi:10.1016/j.cell.2009.06.050

7. Coiro P, Stoenica L, Strauss U, Brauer AU. Plasticity-related gene 5 promotes spine formation in murine hippocampal neurons. *J Biol Chem*. Sep 05 2014;289(36):24956-70. doi:10.1074/jbc.M114.597880

8. Brosig A, Fuchs J, Ipek F, et al. The Axonal Membrane Protein PRG2 Inhibits PTEN and Directs Growth to Branches. *Cell Rep*. Nov 12 2019;29(7):2028-2040 e8. doi:10.1016/j.celrep.2019.10.039

9. Strauss U, Brauer AU. Current views on regulation and function of plasticity-related genes (PRGs/LPPRs) in the brain. *Biochim Biophys Acta*. Jan 2013;1831(1):133-8. doi:10.1016/j.bbalip.2012.08.010

10. Peeva GP, Angelova SK, Guntinas-Lichius O, et al. Improved outcome of facial nerve repair in rats is associated with enhanced regenerative response of motoneurons and augmented neocortical plasticity. *Eur J Neurosci*. Oct 2006;24(8):2152-62. doi:10.1111/j.1460-9568.2006.05091.x

11. Cheng J, Sahani S, Hausrat TJ, et al. Precise Somatotopic Thalamocortical Axon Guidance Depends on LPA-Mediated PRG-2/Radixin Signaling. *Neuron*. Oct 5 2016;92(1):126-142. doi:10.1016/j.neuron.2016.08.035

12. Broggini T, Nitsch R, Savaskan NE. Plasticity-related gene 5 (PRG5) induces filopodia and neurite growth and impedes lysophosphatidic acid- and nogo-A-mediated axonal retraction. *Mol Biol Cell*. Feb 15 2010;21(4):521-37. doi:10.1091/mbc.E09-06-0506

13. Yu P, Agbaegbu C, Malide DA, et al. Cooperative interactions of LPPR family members in membrane localization and alteration of cellular morphology. *J Cell Sci*. Sep 01 2015;128(17):3210-22. doi:10.1242/jcs.169789

14. Sigal YJ, Quintero OA, Cheney RE, Morris AJ. Cdc42 and ARP2/3-independent regulation of filopodia by an integral membrane lipid-phosphatase-related protein. *J Cell Sci*. Jan 15 2007;120(Pt 2):340-52. doi:10.1242/jcs.03335

15. Broggini T, Schnell L, Ghoochani A, et al. Plasticity Related Gene 3 (PRG3) overcomes myelin-associated growth inhibition and promotes functional recovery after spinal cord injury. *Aging (Albany NY)*. Oct 15 2016;8(10):2463-2487. doi:10.18632/aging.101066

16. Velmans T, Battefeld A, Geist B, Farres AS, Strauss U, Brauer AU. Plasticity-related gene 3 promotes neurite shaft protrusion. *BMC Neurosci*. Mar 19 2013;14:36. doi:10.1186/1471-2202-14-36

17. Tanic N, Brkic G, Dimitrijevic B, et al. Identification of differentially expressed mRNA transcripts in drug-resistant versus parental human melanoma cell lines. *Anticancer Res*. May-Jun 2006;26(3A):2137-42.

18. Savaskan NE, Brauer AU, Nitsch R. Molecular cloning and expression regulation of PRG-3, a new member of the plasticity-related gene family. *Eur J Neurosci*. Jan 2004;19(1):212-20.

19. Almagro Armenteros JJ, Tsirigos KD, Sonderby CK, et al. SignalP 5.0 improves signal peptide predictions using deep neural networks. *Nat Biotechnol*. Apr 2019;37(4):420-423. doi:10.1038/s41587-019-0036-z

20. Unichenko P, Kirischuk S, Yang JW, et al. Plasticity-Related Gene 1 Affects Mouse Barrel Cortex Function via Strengthening of Glutamatergic Thalamocortical Transmission. *Cereb Cortex*. Jul 2016;26(7):3260-72. doi:10.1093/cercor/bhw066

21. Wang WZ, Molnar Z. Dynamic pattern of mRNA expression of plasticity-related gene-3 (PRG-3) in the mouse cerebral cortex during development. *Brain Res Bull*. Sep 15 2005;66(4-6):454-60. doi:10.1016/j.brainresbull.2005.05.010

22. Livak KJ, Schmittgen TD. Analysis of relative gene expression data using real-time quantitative PCR and the 2(-Delta Delta C(T)) Method. *Methods*. Dec 2001;25(4):402-8. doi:10.1006/meth.2001.1262

23. Suckau O, Gross I, Schrotter S, et al. LPA1 , LPA2 , LPA4 , and LPA6 receptor expression during mouse brain development. *Dev Dyn*. May 2019;248(5):375-395. doi:10.1002/dvdy.23

Figure Captions

Figure 1: Expression of *Prg* genes during mouse brain development. Analysis of *Prg1-5* mRNA expression in murine hippocampus, neocortex, olfactory bulbs, and cerebellum between E14 and P30 by qRT-PCR. **(A, C, E and G)** Relative mRNA expression normalized to *Gapdh* and shown for each *Prg* over developmental stages. *Prg3* and *Prg5* expression during hippocampus development, which was published in Velmans et al. 2013 and Coiro et al. 2014 is shown in **(A)** in shaded bars. Statistical analysis was performed using a one-way ANOVA followed by Bonferroni's multiple comparisons test. Data are shown as mean ± SD and were considered significant for $p \leq 0.05$ (* $p \leq 0.05$, *** $p \leq 0.01$, ns = not significant). *p* values are listed in Table 1. Embryonic stages: n = 3; N = 21 to 30. Postnatal stages: n = 3; N = 18. **(B, D, F and H)** Change of mRNA expression normalized to birth (P0) expression level. E, embryonic day; P, postnatal day; n = number of independent preparations; N = number of total animals.

Figure 2: Expression of *Prg* genes in primary cultured brain cells. (A) Analysis of *Prg1-5* mRNA expression in primary cultured hippocampal neurons (DIV7), astrocytes (DIV14-16) and microglia (DIV14-16) by qRT-PCR. *Prg3* and *Prg5* mRNA expression were published in Velmans et al. 2013 and Coiro et al. 2014 and are included for comparison (shaded bars). Statistical analysis was performed using a one-way ANOVA followed by a Bonferroni's multiple comparisons test. Data are shown as the relative expression normalized to *Gapdh* as mean ± SD and were considered significant for $p \leq 0.05$ (* $p \leq 0.05$, *** $p \leq 0.01$). Neurons: n = 3; N = 21 to 30. Astrocytes and microglia: n = 3; N = 9 to 12. **(B)** Analysis of *Prg1-5* mRNA expression in immature (DIV3, clear bars) and mature (DIV6, patterned bars) primary cultured oligodendrocytes. Data are shown as the relative expression normalized to *Gapdh* as

mean ± SD. Statistical analysis was performed using a one-tailed *t*-test. Data were considered significant for $p \leq 0.05$ (* $p \leq 0.05$; n = 3; N = 9). n = number of independent preparations; N = number of total animals.

Figure 3: Amino acid sequence alignment of murine PRG3, PRG5, and PRG4, starting from the N-terminus. Differing amino acids are marked in red, transmembrane regions (TM) are highlighted in blue, extracellular loops (ECL) in green; intracellular regions are not highlighted (ICL = intracellular loop). The main differences can be seen in N- and C-termini, the first intracellular loop, and the second extracellular loop. Sequences were aligned using CLC Sequence Viewer 8. Primary accession numbers: Q8BFZ2 (mPRG3), Q8VCY8 (mPRG4), Q8BJ52 (mPRG5).

Figure 4: PRG4-eGFP fusion proteins did not induce filopodial outgrowth in HEK293H cells, and the GFP fusion site plays a role in PRG5 function. Representative images of HEK293H cells transfected with C-terminal eGFP fusion proteins **(A)** and N-terminal eGFP fusion proteins **(B)** of PRG3, PRG4, and PRG5 (green). Cell nuclei were stained with DAPI (blue). Scalebars 20µm. **(C)** Boxplot of number of filopodia per cell after overexpression with C-terminal FLAG-tagged PRG3, PRG4, or PRG5 proteins and the membrane marker CFP-MEM in HEK293H cells. Statistical analysis was performed using a Kruskal-Wallis test followed by a Dunn's multiple comparison test and were considered significant for $p \leq 0.05$ (* $p \leq 0.05$, *** $p \leq 0.01$). n = 3 individual transfection experiments with at least 10 cells per experiment; N = number of total cells.

Figure 5: Co-transfection of PRG3 and PRG5 with PRG4 did not increase its localization to the filopodia plasma membrane. Representative images of HEK293H cells co-transfected with a PRG4-FLAG construct (magenta) and either PRG3-eGFP **(A)** or PRG5-eGFP **(B)** constructs or CFP-MEM **(C)** as a control

membrane protein (green). White arrow heads indicate absence of PRG4 in filopodia and membrane protrusions in higher magnification and orthogonal views. Scalebars 20 µm.

Table 1: Significance and *p* values for one-way ANOVA of *Prg* gene expression during mouse brain development (* $p \leq 0.05$, *** $p \leq 0.01$, ns = not significant).

Table 3: TaqMan™ gene expression assays (FAM/MGB-coupled) used for qRT-PCR.

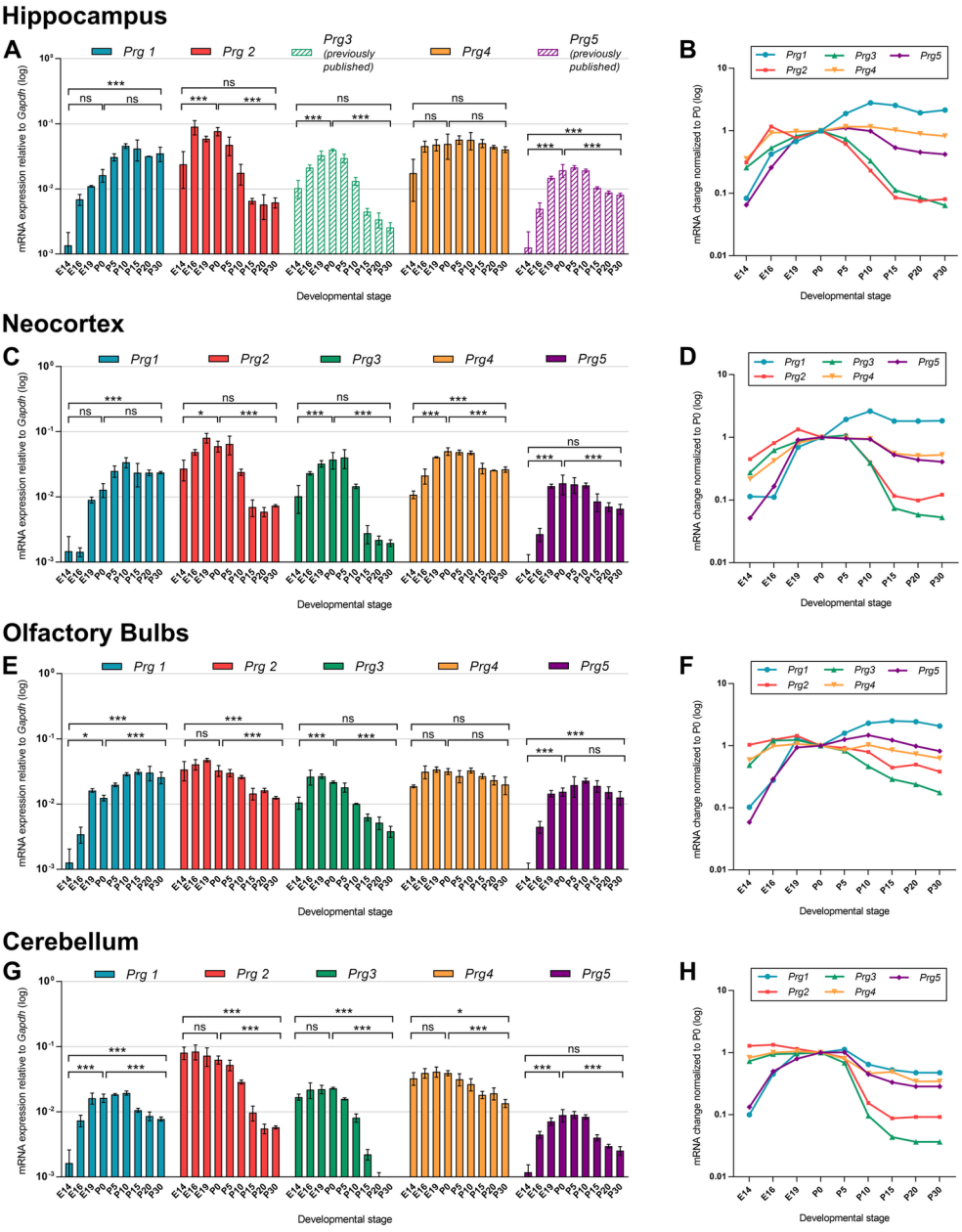

DVDY_428_cc.Figure1.tiff

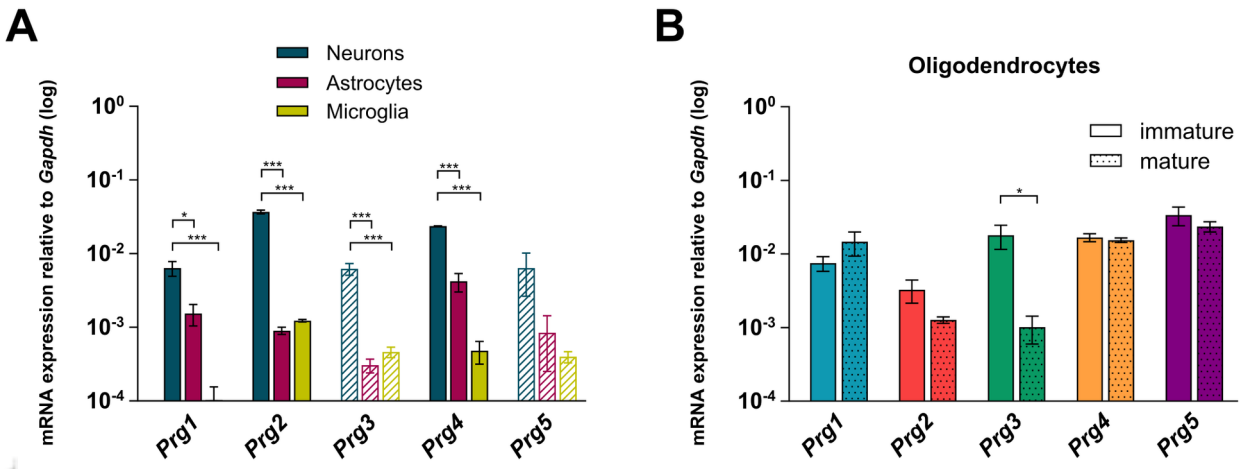

DVDY_428_cc.Figure2.2.tif

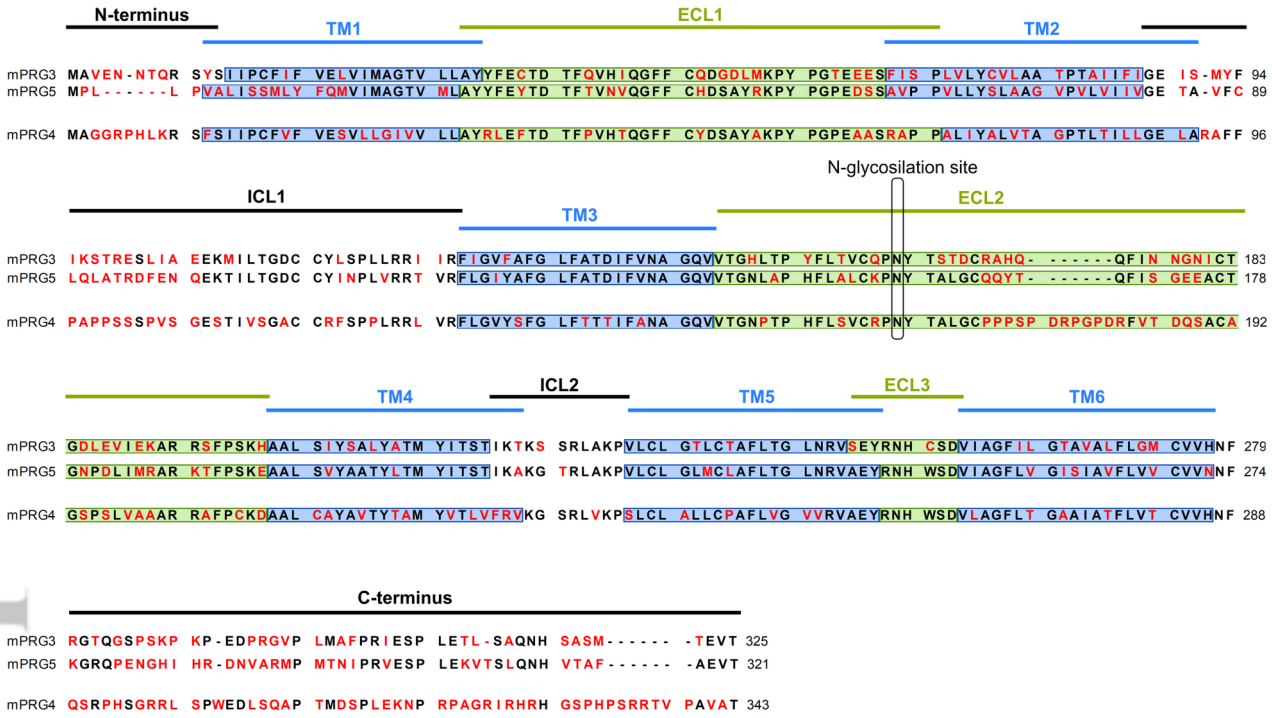

DVDY_428_Figure3.tif

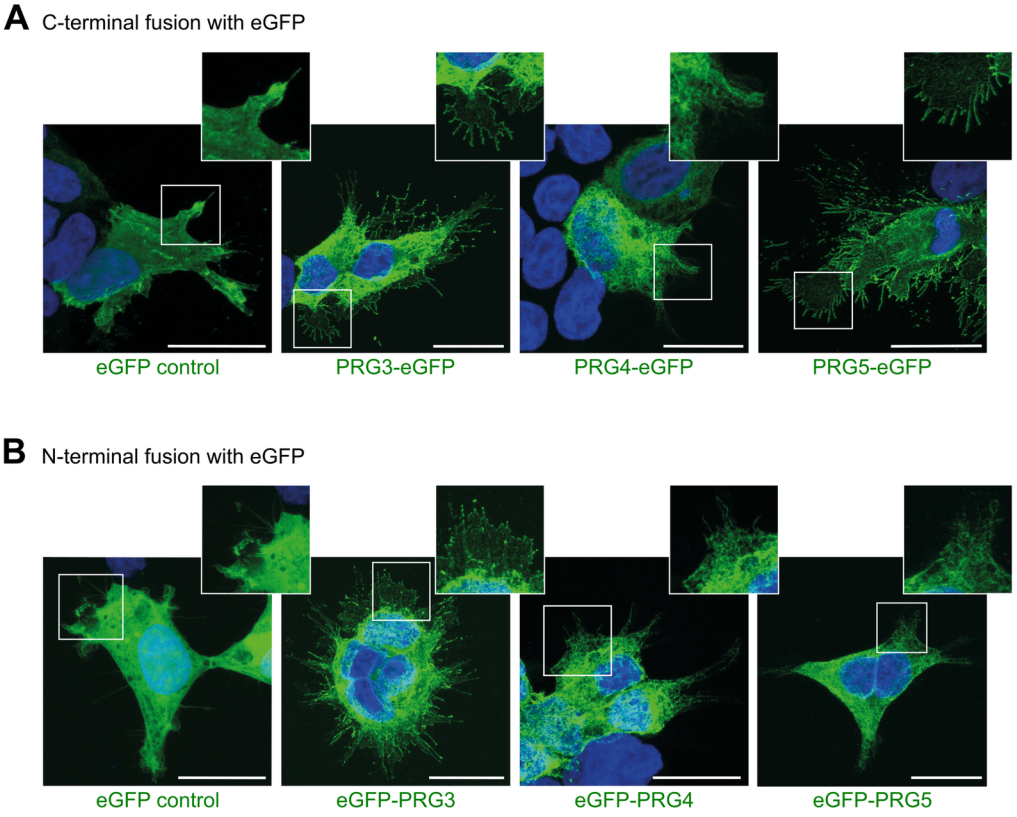

DVDY_428_cc.Figure4.tiff

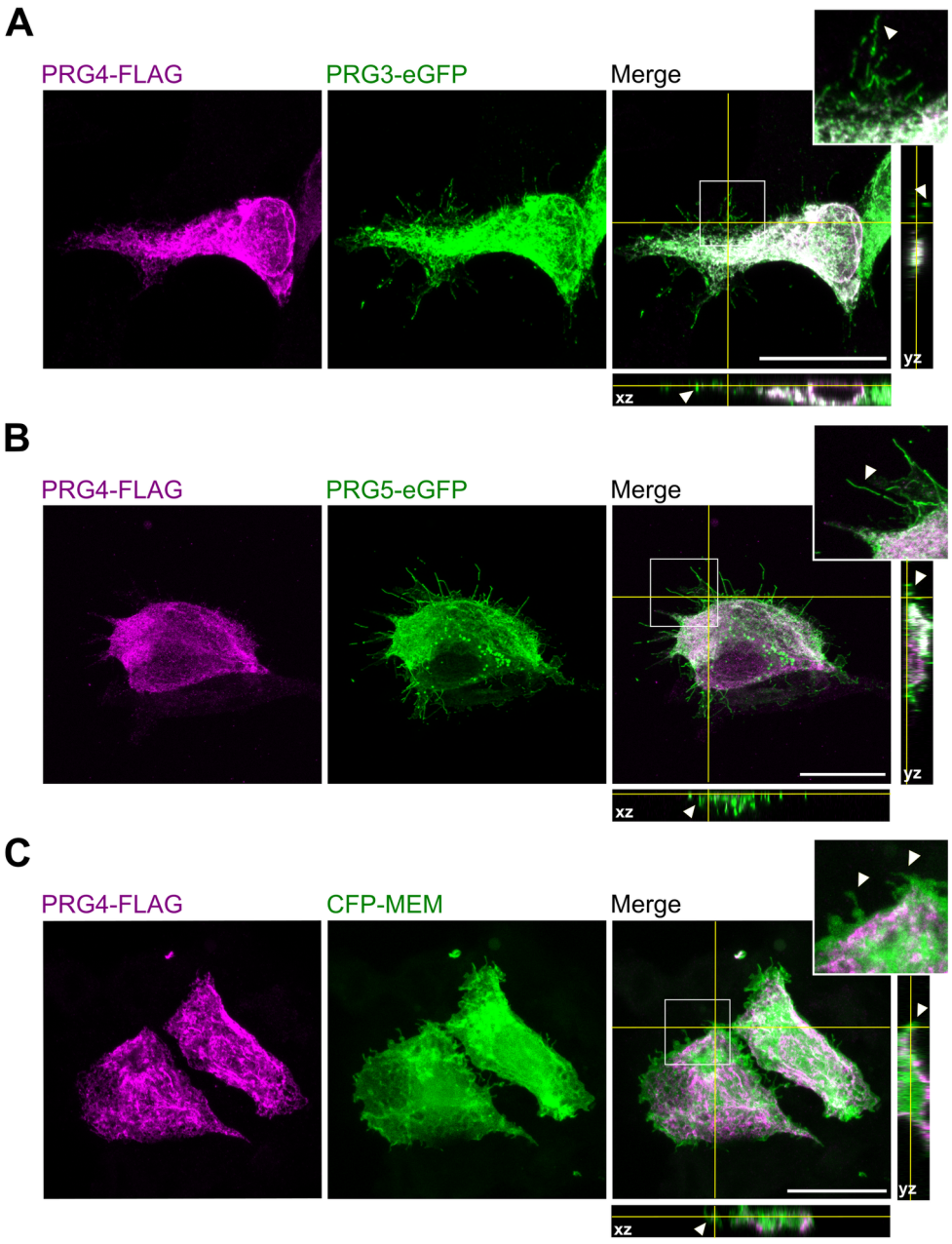

DVDY_428_cc.Figure5.tiff

		Hippocampus		Neocortex		Olfactory Bulbs		Cerebellum	
Prg1	**E14 vs. P0**	ns	0.2977	ns	0.1443	*	0.0255	***	< 0.0001
	P0 vs. P30	ns	0.0577	ns	0.2219	***	0.0043	***	0.0002
	E14 vs. P30	***	0.0001	***	0.0002	***	< 0.0001	***	0.0075
Prg2	**E14 vs. P0**	***	0.0006	*	0.024	ns	> 0.9999	ns	> 0.9999
	P0 vs. P30	***	0.0001	***	0.0001	***	0.007	***	0.0012
	E14 vs. P30	ns	0.9999	ns	0.8663	***	0.004	***	< 0.0001
Prg3	**E14 vs. P0**	***	0.0001	***	0.001	***	0.0036	ns	0.2483
	P0 vs. P30	***	0.0001	***	< 0.0001	***	< 0.0001	***	< 0.0001
	E14 vs. P30	ns	0.1171	ns	> 0.9999	ns	0.2807	***	< 0.0001
Prg4	**E14 vs. P0**	ns	0.1048	***	< 0.0001	ns	0.0562	ns	> 0.9999
	P0 vs. P30	ns	> 0.9999	***	< 0.0001	ns	0.1228	***	0.0006
	E14 vs. P30	ns	0.8021	***	0.0041	ns	> 0.9999	*	0.0147
Prg5	**E14 vs. P0**	***	< 0.0001	***	< 0.0001	***	0.0009	***	< 0.0001
	P0 vs. P30	***	<0,0001	***	0.0088	ns	>0,9999	***	< 0.0001
	E14 vs. P30	***	0.0038	ns	0.494	***	0.0095	ns	> 0.9999

DVDY_428_cc.Table1.tif

Gene	Organism	Assay-ID / primer and probe sequence (self-designed probes)
Gapdh, glyceraldehyde-3-phosphate dehydrogenase	*Mus musculus* (mouse)	Mm99999915_g1
Actb, beta-actin	*Mus musculus* (mouse)	Mm00607939_s1
Prg1 (Lppr4), plasticity-related gene 1	*Mus musculus* (mouse)	Mm00724102_m1
Prg2 (Lppr3), plasticity-related gene 2	*Mus musculus* (mouse)	GenBank Accession-Nr.: NM_144935 Forward primer (5'-3'): CCTCCGGCGCACAGT Reverse primer (5'-3'): AGAGCCGTGGCACACA TaqManTM Probe (5'-3'): ACACGTGTACACCCACAAAG
Prg3 (Lppr1), plasticity-related gene 3	*Mus musculus* (mouse)	Mm00626670_m1
Prg4 (Lppr2), plasticity-related gene 4	*Mus musculus* (mouse)	Mm00460726_m1
Prg5 (Lppr5), plasticity-related gene 5	*Mus musculus* (mouse)	Mm01310525_m1

DVDY_428_cc.Table3.tif